Sussex Research Online

Improvement of contact resistance in flexible a-IGZO thin-film transistors by CF4/O2 plasma treatment

Article (Accepted Version)

Improvement of Contact Resistance in Flexible a-IGZO Thin-film Transistors by CF4/O2 Plasma Treatment

S. Knobelspies[a], A. Takabayashi[b], A. Daus[a], G. Cantarella[a], N. Münzenrieder[a,c], and Gerhard Tröster[a]

[a] *Institute for Electronics, Swiss Federal Institute of Technology Zurich, Zurich 8092, Switzerland.*
[b] *Institut de microtechnique, Ecole Polytechnique Federale de Lausanne, 1015 Lausanne, Switzerland.*
[c] *Sensor Technology Research Center, School of Engineering and Informatics, University of Sussex, Falmer, Brighton BN1 9QT, UK.*

Abstract

In this work, we analyze the effect of CF4/O2 plasma treatment on the contact interface between the amorphous Indium-Gallium-Zinc-Oxide (a-IGZO) semiconductor and Titanium-Gold electrodes. First, the influence of CF4/O2 plasma treatment is evaluated using transmission line structures and compared to pure O2 and CF4 plasma, resulting in a reduction of the contact resistance RC by a factor of 24.2 compared to untreated interfaces. Subsequently, the CF4/O2 plasma treatment is integrated in the a-IGZO thin-film transistor (TFT) fabrication process flow. We achieve a reduction of the gate bias dependent RC by a factor up to 13.4, which results in an increased current drive capability. Combined with an associated channel length reduction, the effective linear field-effect mobility $\mu_{\text{lin,FE,eff}}$ is increased by up to 74.6% for the CF4/O2 plasma treated TFTs compared to untreated reference devices.

Keywords: a-IGZO, flexible electronics, thin-film transistor, contact resistance, plasma treatment, CF4.

1. Introduction

Flexible thin-film transistors (TFTs) attract remarkable attention in applications such as flexible displays [1], electronic papers [2] or sensors [3]. To integrate these flexible devices into wireless technology, the TFT is required

to operate in the megahertz regime to process and transmit signals [4]. Possible channel materials are e.g., 2D semiconductors [5], carbon nanotubes [6] or amorphous oxide semiconductors (AOS). The latter ones show excellent properties, such as high uniformity, large area processability, long-term stability and the possibility for room temperature fabrication [7]. In the field of applicable AOS, amorphous InGaZnO (a-IGZO) exhibits exceptional electronic characteristics, such as an electron mobility greater than 10 cm^2/Vs, low off current and already became commercially viable [7, 8, 9].

The speed of a TFT can be quantified by the transit frequency ft [10]. Although this parameter is linearly dependent on the field-effect mobility and quadratically dependent on the transistor channel length, downscaling of the TFT dimensions will not necessarily result in an increase of ft. Short channel effects, the parasitic overlap capacitance COV and a dominating contact resistance RC limit the device performance [4]. Several efforts have been undertaken to reduce COV, e.g., by self-alignment techniques [10] or stripe-patterned electrodes [11].

In this work, we focus on improving the RC between semiconductor (a-IGZO) and Ti/Au source/drain electrodes. It is known from gate bias dependent RC measurements that the RC in TFTs depends on the number of charge carriers in the a-IGZO film [12]. Several groups have shown, that various plasma treatments (i.e. NH3 [17], Ar [18, 19, 20, 21, 22, 23], N2 [20], NF3 [24], He [18, 25], O2 [20], N2O [26], H2 [22] and recently F [27]) can change the electrical characteristics and e.g., form heavily doped n$^+$ a-IGZO. So far, there is no report on the effects of CF4/O2 plasma and, to the best of our knowledge, we apply for the first time a CF4 based plasma treatment on the contact areas of a-IGZO TFTs to investigate the contact resistance. Therefore, we studied in a first approach the effect of this treatment (applied on the contact interface) on the contact resistance RC between semiconductor and a-IGZO by using the transmission line method (TLM) [14] and compare it to pure CF4 and O2 plasma treatments. Afterwards, the CF4/O2 plasma treatment is applied to flexible a-IGZO based TFTs. The results show that the gate bias dependent RC is significantly lowered throughout the whole operation regime. Furthermore, we observe a channel length reduction which leads, in combination with the lowered RC, to an increase of the extracted effective linear field-effect mobility $\mu_{\mathrm{lin,FE,eff}}$. Our proposed plasma treatment can be directly implemented into the fabrication process of flexible a-IGZO TFT technology, thus paving the way for high frequency operation and increased drive currents of a-IGZO TFTs and even short channel devices, while
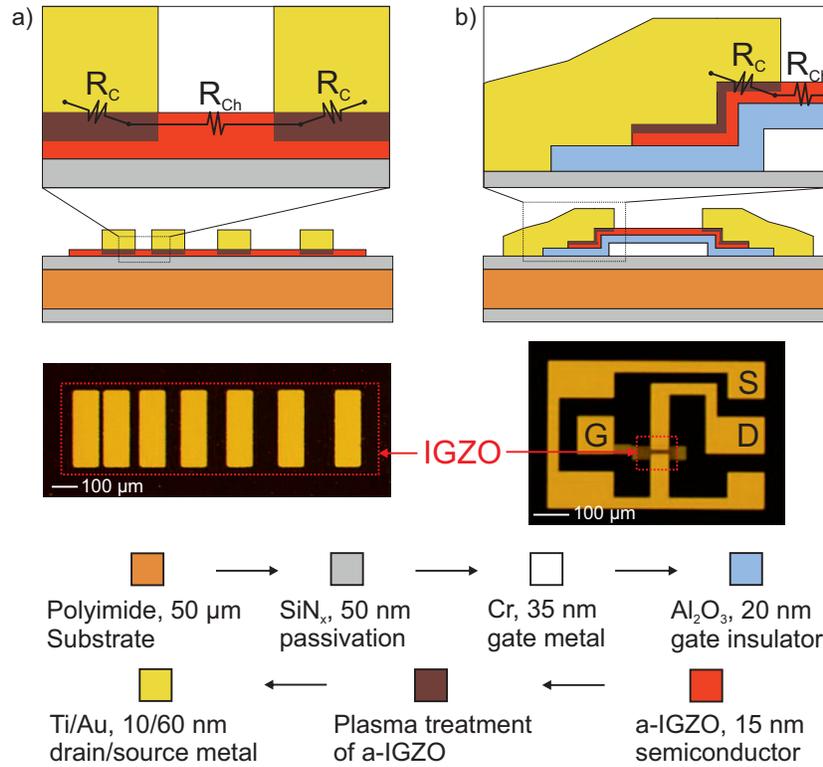
2

Figure 1: Schematic cross section and microscopic image of the devices: a) Transmission line structure and b) thin-film transistor. The schematic fabrication process is sketched in the flow chart. The magnified areas highlight the plasma treated contact interfaces (a-IGZO: red; plasma treated a-IGZO: brown), the contact resistance RC and the channel resistance RCh.

still utilizing standard UV lithography methods.

2. Experimental

2.1. Fabrication

The TLM structures and TFTs are fabricated on free-standing 50 µm thick flexible plastic foils (Kapton E, DuPont). The substrates are cleaned in Acetone and 2-Propanol for 5 minutes each with the help of ultrasonic treatment. Subsequently a bakeout at 200 °C for 24 hours is performed to remove residual solvents. The substrate is passivated with 50 nm SiNx by plasma-enhanced chemical vapor deposition on both sides to promote the adhesion of the following layers.

2.1.1. TLM structure fabrication

15 nm a-IGZO is RF magnetron sputtered at room temperature. Then, MaN-1420 photoresist is spin-coated and structured by photolithography to prepare the lift-off process for the electrodes. At this point the plasma treatment is performed and subsequently, the Ti/Au (10/60 nm) electrode layer is electron-beam (e-beam) evaporated on the sample. After structuring the electrodes by lift-off, the a-IGZO is patterned into islands by photolithography and wet chemical etching.

2.1.2. TFT fabrication

30 nm Cr is e-beam evaporated onto the substrate and structured by lithography and wet chemical etching. A 20 nm thick Al2O3 gate insulator layer is grown by thermal atomic-layer deposition at 150 °C. Then, 15 nm a-IGZO is deposited as described in the previous section. The a-IGZO is structured into islands and vias are formed in the gate insulator, both by photolithography and wet chemical etching. Then, similar to the TLM structures, MaN-1420 photoresist is spin-coated and structured by photolithography followed by the plasma treatment. The Ti/Au (10/60 nm) electrode layer is deposited by e-beam evaporation. Therefore, the plasma treated a-IGZO area is self-aligned with the deposited Ti/Au electrodes.

A schematic cross section and a microscopic image of both devices (including a magnified area to highlight the plasma treated areas), and the fabrication process flow, are presented in Figure 1a and 1b.

2.2. Plasma treatment

The duration of all plasma treatments is 1 min, the pressure 133 µbar and the RF power 150 W. The gas compositions are shown in Table 1. Negative photoresist is used as mask because of its typically higher mechanical and chemical stability compared to positive photoresist.

3. Results and discussion

3.1. TLM results

The TLM structure electrodes have a width W = 300 µm and length L = 100 µm (see Figure 1a). The spacing d between the contact pads is varied from 20 to 120 µm. By measuring the resistance Rtot between two neighboring electrodes in relation to d, 2·RC can be extrapolated at the intersection with the y-axis. Table 1 compares the extracted mean 2·RC and

Table 1: TLM contact resistance RC with sample size N=6 each.

Plasma composition	mean 2·RC	std. error of mean
Pure O2	$1.35 \cdot 10^{11}\Omega$	$9.56 \cdot 10^{9}\Omega$
Untreated	$5.45 \cdot 10^{10}\Omega$	$1.01 \cdot 10^{10}\Omega$
Pure CF4	$2.45 \cdot 10^{10}\Omega$	$4.83 \cdot 10^{9}\Omega$
CF4/O2 (10:1)	$2.28 \cdot 10^{9}\Omega$	$4.45 \cdot 10^{8}\Omega$

their standard errors for CF4/O2, CF4 and O2 plasma treated and untreated samples.

Pure O2 plasma treatment results in an increased RC, while pure CF4 plasma treatment shows a reduced RC compared to the untreated reference sample. However, it is known that pure CF4 plasma can lead to polymerization effects on the surface [13], thus resulting in a non-ideal interface. Therefore, a small ratio of O2 is added to counteract this phenomena while not canceling the positive effect of CF4 on the RC. With the combined CF4/O2 plasma, we obtain an improved RC by a factor of 24.2 compared to the reference. Fluorine can substitute O lattice sites and occupy O vacancies at the a-IGZO surface, thus generating free electrons and reducing the number of electron traps [24, 27]. We believe that the formation of a thin layer of highly doped a-IGZO (with increased number of charge carriers) leads to field emission (charge carrier tunnel through the potential barrier) [15], which results in the decreased RC. The change in a-IGZO conductivity is confirmed after applying CF4 plasma on the area between the electrodes and observing a conductivity increase by a factor of 10^{4}, which is in agreement on studies about F doped a-IGZO [27]. Previous reports presented the incorporation of F into a-IGZO with a post-annealing at 450 °C, leading to the formation of highly conductive a-IGZO [16]. In our case, the plasma delivers the necessary energy to activate this transition, which allows this treatment to be integrated into the TFT fabrication routine on flexible polyimide. Consequently, the plasma treatment is applied on a-IGZO based TFTs to investigate the VGS dependent RC.

3.2. TFT results

TFTs with untreated and CF4/O2 plasma treated source/drain-IGZO contact areas are fabricated and the transfer (drain current ID vs. gate-
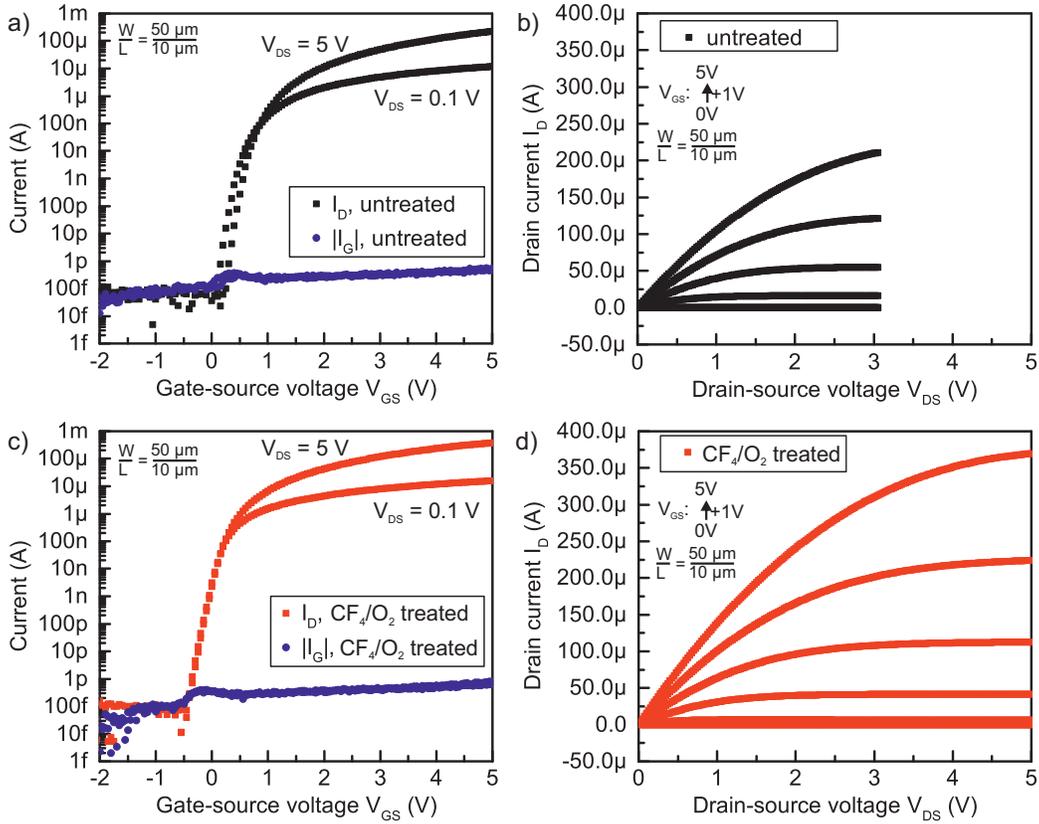
Figure 2: a) Transfer and b) output curves of the untreated a-IGZO TFT. c) Transfer and d) output characteristic of the CF4/O2 plasma treated a-IGZO TFT.

source voltage VGS) and output (ID vs. drain-source voltage VDS) characteristics are measured. All devices have a channel width W = 50 µm and a source/drain to gate overlap length of 15 µm. The electrical parameters are extracted using the Y-function method [28], which uses the combination of the ID- and transconductance transfer curves. Figure 2 presents two exemplary ID-VGS and ID-VDS curves for 10 µm long untreated and CF4/O2 treated TFTs. Both TFTs show a saturating behavior. The output curves indicate an increased ID for the CF4/O2 treated TFT, while the VTh is negatively shifted (see transfer curves; mean VTh shift of −0.52 V). Nevertheless, when comparing the ID values at the same overdrive voltage VOV=VGS-VTh, the CF4/O2 treated TFT still shows an improved current drive capability (factor of 1.24 at VOV = 3 V). Both devices show similar

gate currents and the ON/OFF ratio is above 10^8 for all TFTs. To further analyze the RC, the ID-VGS curves are used to extract the VOV-dependent RC. As shown in Figure 3a, we observe a significantly lowered RC for CF4/O2 treated contacts (by a factor of 13.4 ± 2.2 in the whole VOV regime), as well as the typical trend of RC with varying VOV [12]. To give an impression about the accuracy of the extracted RC values, the respective adjusted R^2 values are plotted in Figure 3b. Therefore, the increased TFT ID can be attributed to the decreased RC.
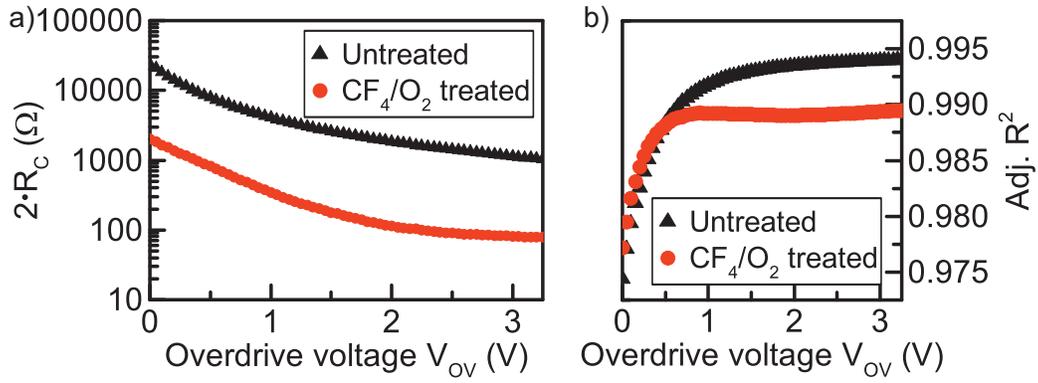

Figure 3: a) Overdrive voltage VOV dependent contact resistance 2·RC of untreated and CF4/O2 treated a-IGZO TFTs. b) The adjusted R^2-values of the 2·RC values extracted from 5 individual TFTs per data point.

Figure 4 presents the $\mu_{\text{lin,FE,eff}}$ and the transconductance gm at VOV = 3 V for untreated and CF4/O2 treated TFTs at in relation to their channel length L. For L $\geq$ 5 µm, the $\mu_{\text{lin,FE,eff}}$ is increased by 16.7 % to 23.6 %. For L < 5 µm, the $\mu_{\text{lin,FE,eff}}$ increases significantly by 74.6 %. We attribute this enormous increase to a reduction of the effective channel length by ΔL. The negative photoresist, which is used as a mask for the plasma treatment and the lift-off process forms an undercut structure during development. Therefore, the plasma may also change the conductivity of a small portion of the transistor channel. The ΔL is extracted as 0.7 µm, according to the method described in [29]. This effect has a significant influence on short-channel TFTs, while it becomes less significant for longer channel lengths. This effect can be utilized for the fabrication of flexible short channel TFTs with standard UV lithography, where the minimum feature size will not limit the minimum channel length any more.
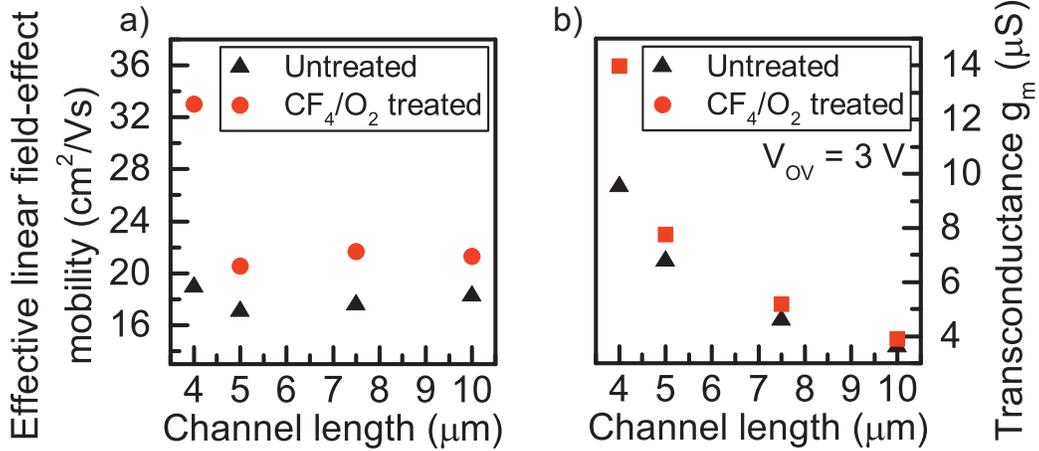
Figure 4: a) Effective linear field-effect mobility $\mu_{\mathrm{lin,FE,eff}}$ extracted by the Y-function method and b) transconductance g_m of untreated and CF4/O2 plasma treated a-IGZO TFTs at VOV = 3 V.

4. Conclusion

In summary, we presented a method to reduce the contact resistance between a-IGZO and Ti/Au, that is suitable for integration into standard flexible TFT fabrication. By CF4/O2 plasma treatment of the a-IGZO layer interfacing with the Ti/Au electrodes, a highly conductive a-IGZO area is formed (i.e., an area with increased charge carrier density). From TLM measurements, we observed a reduction of RC by a factor of 24.2. The implementation of the plasma treatment into the TFT fabrication flow resulted in a reduction of the VOV dependent RC by a factor of 13.4 ± 2.2 over the whole VOV regime and an associated increase in gm and $\mu_{\mathrm{lin,FE,eff}}$. We believe that the proposed technique can be applied in combination with other source/drain metalizations to effectively reduce the RC. Additionally, the observed channel length reduction can be utilized to fabricate short-channel TFTs with standard UV lithography methods, while counteracting short-channel problems, such as a dominant RC in comparison to the channel resistance. Nevertheless, to fully analyze the effect of our proposed plasma treatment, the impact of different plasma parameters, such as RF Power and duration need to be further exploited.

5. Acknowledgements

References

[1] Niu Y, Liu S-F, Chiou J-Y, Huang C-Y, Chiu Y-W, Lai M-H, et al. Improving the flexibility of AMOLED display through modulating thickness of layer stack structure. J Soc Inf Disp. 2016;24(5):2938.

[2] Shishido H, Amano S, Toyotaka K, Miyake H, Murakawa T. 28.2: Color Sequential LC Display Using High Reliable Oxide Semiconductors with Monochrome Electronic Paper Function. SID Symp Dig Tech Pap. 2011;42(1):36972.

[3] Knobelspies S, Bierer B, Daus A, Takabayashi A, Salvatore GA, Cantarella G, et al. Photo-induced room-temperature gas sensing with a-IGZO based thin-film transistors fabricated on flexible plastic foil. Sensors (Switzerland). 2018;18(2):358.

[4] Münzenrieder N, Salvatore GA, Petti L, Zysset C, Büthe L, Vogt C, et al. Contact resistance and overlapping capacitance in flexible sub-micron long oxide thin-film transistors for above 100 MHz operation. Appl Phys Lett. 2014;105(26):263504.

[5] Akinwande D, Petrone N, Hone J. Two-dimensional flexible nanoelectronics. Nat Commun. Nature Publishing Group; 2014;5:112.

[6] Sun DM, Timmermans MY, Tian Y, Nasibulin AG, Kauppinen EI, Kishimoto S, et al. Flexible high-performance carbon nanotube integrated circuits. Nat Nanotechnol. Nature Publishing Group; 2011;6(3):15661.

[7] Fortunato E, Barquinha P, Martins R. Oxide semiconductor thin-film transistors: A review of recent advances. Adv Mater. 2012;24(22):294586.

[8] Nomura K, Ohta H, Takagi A, Kamiya T, Hirano M, Hosono H. Room-temperature fabrication of transparent flexible thin-film transistors using amorphous oxide semiconductors. Nature. 2004;432(7016):48892.

[9] Sharp. Sharp Begins Production of Worlds First LCD Panels Incorporating IGZO Oxide Semiconductors. Press Releases [Internet]. 2012 Apr 13; Available from: http://www.sharp-world.com

[10] Münzenrieder N, Petti L, Zysset C, Kinkeldei T, Salvatore GA, Tröster G. Flexible self-aligned amorphous InGaZnO thin-film transistors with submicrometer channel length and a transit frequency of 135 MHz. IEEE Trans Electron Devices. 2013;60(9):16.

[11] Lee S, Chen Y, Jeon J, Park C, Jang J. Reduction of Parasitic Capacitance in Indium-Gallium-Zinc Oxide (a-IGZO) Thin-Film Transistors (TFTs) without Scarifying Drain Currents by Using Stripe-Patterned Source / Drain Electrodes. Adv Electron Mater. 2018;1700550.

[12] Wang W, Li L, Lu C, Liu Y, Lv H, Xu G, et al. Analysis of the contact resistance in amorphous InGaZnO thin film transistors. Appl Phys Lett. 2015;107(6):063504.

[13] Stoffels WW, Stoffels E, Tachibana K. Polymerization of fluorocarbons in reactive ion etching plasmas. J Vac Sci Technol A Vacuum, Surfaces, Film. 1998;16(1):87.

[14] Reeves GK, Harrison HB. Obtaining the Specific Contact Resistance from Transmission Line Model Measurements. IEEE Electron Device Lett. 1982;3(5):1113.

[15] Rhoderick EH. Metal-semiconductor contacts. IEE Proc I - Solid-State Electron Devices. 1982;129(1):1.

[16] Lu L, Xia Z, Li J, Feng Z, Wang S, Kwok HS, et al. A Comparative Study on Fluorination and Oxidation of Indium-Gallium-Zinc Oxide Thin-Film Transistors. IEEE Electron Device Lett. 2017;39(2):1969.

[17] Kim S, Park J, Kim C, Song I, Kim S, Park S, et al. Source/drain formation of self-aligned top-gate amorphous GaInZnO thin-film transistors by NH3 plasma treatment. IEEE Electron Device Lett. 2009;30(4):3746.

[18] Magari Y, Makino H, Furuta M. Carrier generation mechanism and origin of subgap states in Ar- and He-plasma-treated InGaZnO thin films. ECS J Solid State Sci Technol. 2017;6(8):Q1017.

[19] Huang XD, Song JQ, Lai PT. Improved Performance of Scaled-Down a-InGaZnO Thin-Film Transistor by Ar Plasma Treatment. IEEE Electron Device Lett. 2016;37(12):15747.

[20] Kim JS, Joo MK, Xing Piao M, Ahn SE, Choi YH, Jang HK, et al. Plasma treatment effect on charge carrier concentrations and surface traps in a-InGaZnO thin-film transistors. J Appl Phys. 2014;115(11):114503.

[21] Park J, Song I, Kim S, Kim S, Kim C, Lee J, et al. Self-aligned top-gate amorphous gallium indium zinc oxide thin film transistors. Appl Phys Lett. 2008;93(5):053501.

[22] Du Ahn B, Shin HS, Kim HJ, Park J-S, Jeong JK. Comparison of the effects of Ar and H2 plasmas on the performance of homojunctioned amorphous indium gallium zinc oxide thin film transistors. Appl Phys Lett. 2008;93(20):203506.

[23] Park JS, Jeong JK, Mo YG, Kim HD, Kim S Il. Improvements in the device characteristics of amorphous indium gallium zinc oxide thin-film transistors by Ar plasma treatment. Appl Phys Lett. 2007;90(26):262106.

[24] Lee S, Shin J, Jang J. Top Interface Engineering of Flexible Oxide Thin-Film Transistors by Splitting Active Layer. Adv Funct Mater. 2017;27(11):19.

[25] Jeong HY, Lee BY, Lee YJ, Lee J Il, Yang MS, Kang IB, et al. Coplanar amorphous-indium-gallium-zinc-oxide thin film transistor with He plasma treated heavily doped layer. Appl Phys Lett. 2014;104(2):022115.

[26] Liang T, Zhang X, Zhou X. Effects of N2O Plasma Treatment Time on the Performance of Self-Aligned Top-Gate amorphous oxide Thin Film Transistors. SID Symp Dig Tech Pap. 2017;48(1):1299302.

[27] Um JG, Jang J. Heavily doped n-type a-IGZO by F plasma treatment and its thermal stability up to 600 C. Appl Phys Lett. 2018;112:162104.

[28] He J, Zhang X, Wang Y, Huang R. New method for extraction of MOSFET parameters. IEEE Electron Device Lett. 2001;22(12):5979.

[29] Kim M-M, Kim M-H, Ryu S -m., Lim JH, Choi D-K. Coplanar ho-
mojunction a-InGaZnO thin film transistor fabricated using ultraviolet
irradiation. RSC Adv. Royal Society of Chemistry; 2015;5(101):8294751.